

ANALYTICAL AND NUMERICAL APPROACH OF LOAD CARRYING CAPACITY FOR PARTIALLY TEXTURED SLIDER

Mircea D. PASCOVICI, Victor MARIAN, Daniel GAMAN

*Department of Machine Elements and Tribology,
Polytechnic University of Bucharest, ROMANIA,
mircea@meca.omtr.pub.ro*

ABSTRACT

Partially textured slider generates load carrying capacity in a similar manner with stepped bearing. The present paper presents a theoretical investigation of a partially textured slider using both analytical and numerical approaches. The pressure distribution is calculated analytically and numerically and the performance of the bearing is evaluated varying different parameters: number of dimples, texture density, dimple depth and textured fraction of the slider. The optimal configuration for the slider is determined in order to produce the highest maximum pressure and thus maximal load carrying capacity.

NOMENCLATURE

a	“active” length of textured zone	p_{max}	slider maximum pressure
b	length of untextured zone	\bar{p}	dimensionless pressure, $\frac{p \cdot h^2}{\eta \cdot U \cdot L_{tot}}$
h	film thickness on the land	s	dimple depth
H	dimensionless film thickness, $\frac{h+s}{h}$	U	sliding velocity
λ	dimple side length	α	textured fraction, $\frac{L_t}{L_{tot}}$
L	cell side length	β	untextured fraction, $\frac{b}{L}$
L_t	textured length	η	viscosity of the lubricant
L_{tot}	total length of the slider	Λ	dimensionless length of lands, $\frac{L-\lambda}{L}$
N	number of dimples on one row	ρ	texture density, $\left(\frac{\lambda}{L}\right)^2$
p	manometric pressure		
p_b	pressure gain on each cell		
p_c	cavitation pressure		
p_i	pressure at the frontier between two adjacent rows		
p_m	local maximum pressure		
p_m^m	mean local pressure		

1. INTRODUCTION

The idea of surface texturing began around 1965 when a solution for generating a self-sustaining film between parallel surfaces was proposed for mechanical seals [8].

This concept was developed after 1990 using primarily the laser technology. Surface texturing found a large number of industrial applications. In the case of mechanical seals this technology enhances the axial stiffness [2, 3, 4, 6]. By texturing the piston rings or the cylinder liner of internal combustion engines, the friction force can be diminished up to 30% [7, 9, 11].

Partially textured thrust bearings have been also manufactured by laser techniques. The pressure distribution of these bearings was theoretically and experimentally investigated for spherical dimples [1, 5].

In the present paper a partially textured slider having dimples of square shape is investigated. The slider can be textured by lithography; the advantage of this technique consists in a reduction of the time needed for texturing.

2. ANALYTICAL MODEL

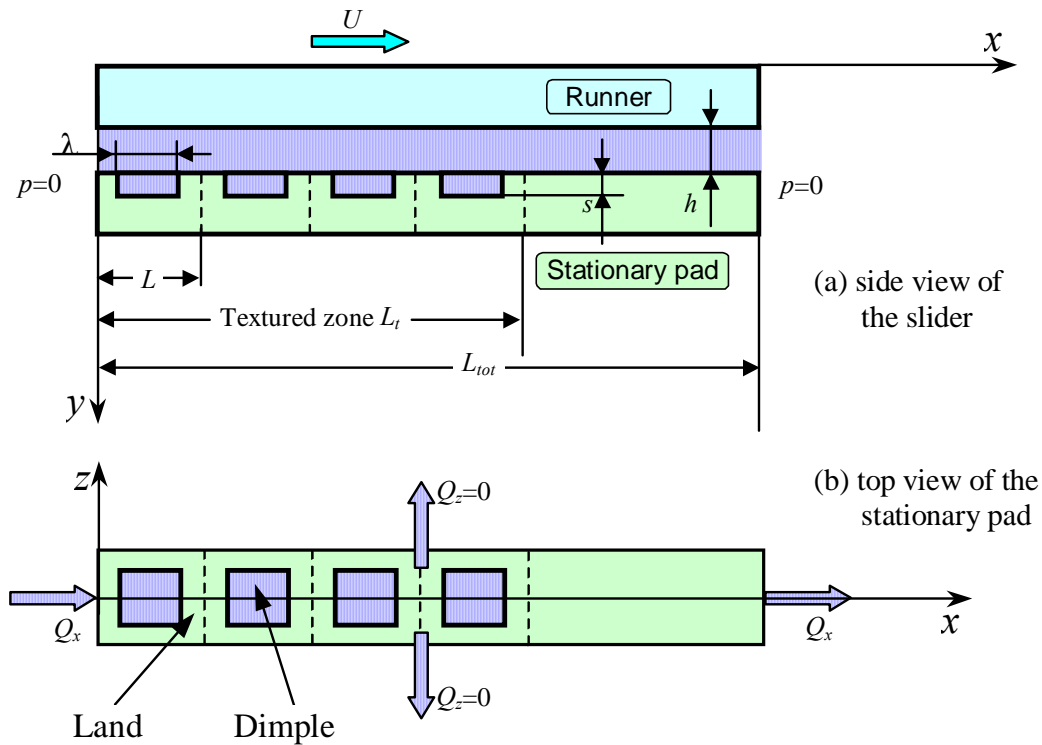


Figure 1 – The geometry of the model

For the sake of simplicity the slider is considered infinitely wide, so only one row will be analyzed with zero flow in z direction (see Figure 1). The manometric pressure at the inlet and outlet of the slider is considered to be zero.

The following main assumptions are considered:

- The lubricant is a Newtonian liquid in laminar and isothermal flow;
- Only one row of dimples is analyzed with zero flow on the sides;
- The pressure distribution on the longitudinal direction on each land and dimple is linear;
- All usual assumptions for thin film lubrication are valid.

The geometry of the model and the assumed pressure distribution is presented in Figure 2. If the textured zone begins with a land, then, according to the conservation of longitudinal rate of flow (Q_x) the pressure gradient must be negative on the first dimple. In other words the Poiseuille rate of flow must introduce lubricant in the first cell. Thus, the cavitation is implicitly considered. However, the cavitation pressure, p_c is relatively small in comparison with the other pressure components (p_b, p_i, p_m, p_{max} , see Figure 2) and for reasons of simplicity of the computation a “shifted” pressure distribution (plotted with dashed line) will be considered. This pressure distribution is similar with that one encountered for spiral groove thrust bearings. In the present case on the first land (the OO' segment in Figure2), the pressure will be considered zero, assumption used for the divergent zone in other lubrication problems such as journal bearings. The results obtained using this approximation will be subsequently rectified by identifying the cavitation pressure, p_c , leading, thus, to the “real” pressure distribution (plotted with continuous line in Figure 2).

Using the pressure distribution sketched in Figure 2 and the similitude of the triangles $\Delta O'CD \sim \Delta O'FB'$ we have:

$$\frac{p_{max} - p_m}{p_b} = \frac{a}{L} \quad (1)$$

The similitude of triangles ΔABC and $\Delta A'B'C$ gives:

$$\frac{p_{max}}{p_m - \Lambda p_b} = \frac{b}{L - \lambda} \quad (2)$$

Combining equations (1) and (2) and introducing dimensionless parameters, we obtain:

$$p_{max} = p_m \frac{\beta N}{\Lambda(N + \beta - \Lambda)} \quad (3)$$

and

$$p_b = p_m \frac{\beta - \Lambda}{\Lambda(N + \beta - \Lambda)} \quad (4)$$

A virtual flow rate balance at the cell level in the local maximum pressure area will be considered for taking in consideration the recirculated flow:

$$Q_z/2 = Q'_x/2 + Q''_x/2=0 \quad (5)$$

Assuming parabolic pressure distribution in z direction and remembering the condition of zero side flow at the boundary between two adjacent rows of dimples, results:

$$\left. \frac{dp}{dz} \right|_{z=0} = - \frac{2(p_m - p_i)}{L - \lambda} \quad (6)$$

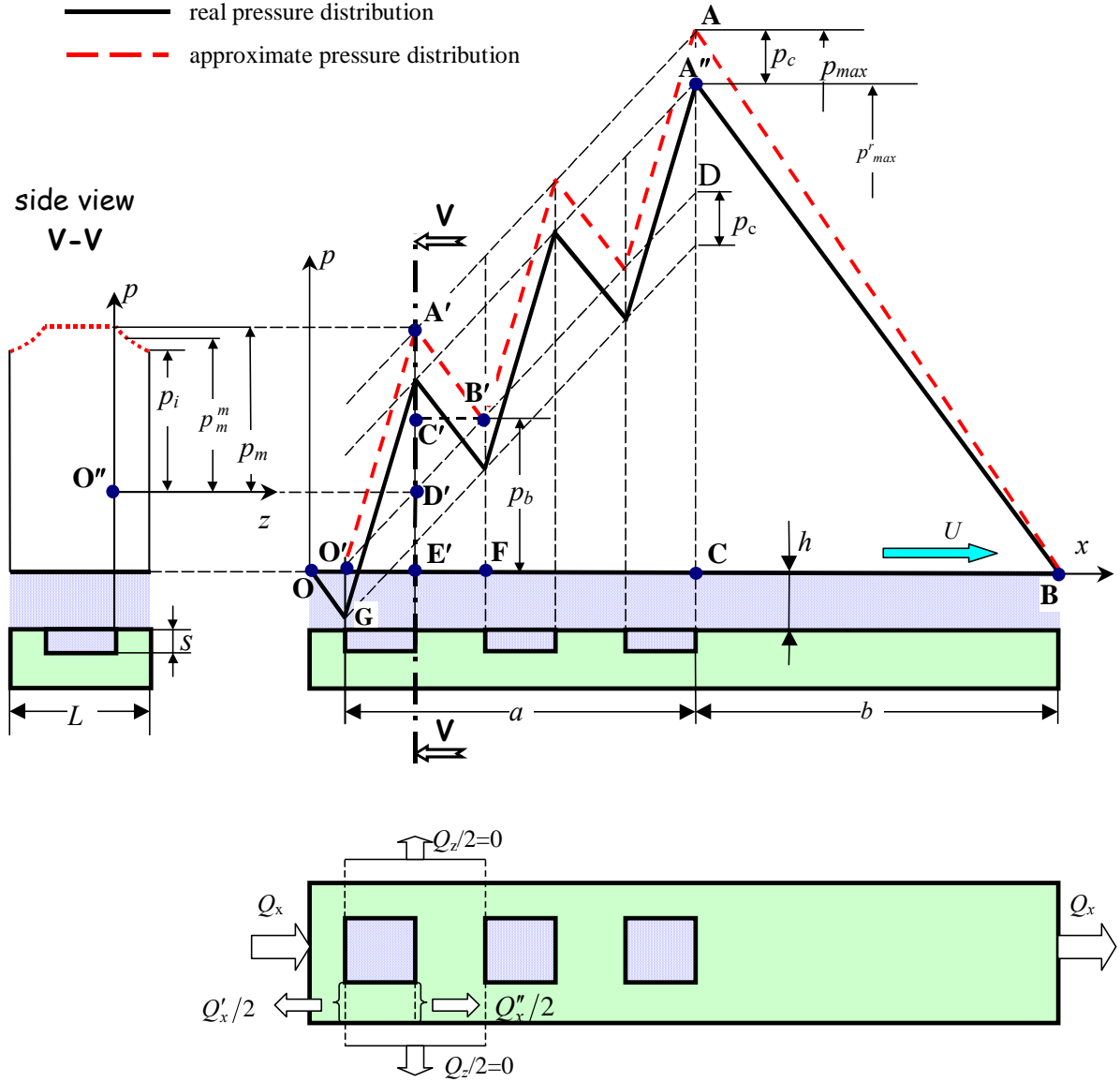


Figure 2 – Geometry and assumed pressure distribution

Between the mean pressure p_m^m and, the pressure at the extremities of parabolic distribution (see Figure 2), p_m and p_i , we have the following relationship:

$$p_i = \frac{3p_m^m - p_m}{2} \quad (7)$$

Finally we obtain the key relationship between mean and maximum local pressures:

$$p_m^m = p_m \frac{6(1-\Lambda)}{6-5\Lambda} \quad (8)$$

Recently, a number of researchers [9,12,13] have found that slip can occur with special engineered surfaces.

For this reason, in the present paper, two different boundary conditions will be considered for the flow modeling:

- In the first case - case A- we assume that the fluid adheres to the surfaces of the slider on the entire extent of the film (**no-slip condition**, typical assumption in fluid dynamics).
- In the second case- case B- we assume that the fluid slips on the bottom of the dimples due to special surface treatments (physical or chemical). However, the no-slip condition remains valid on the lands of the stationary surface and on the runner surface (Figure 3).

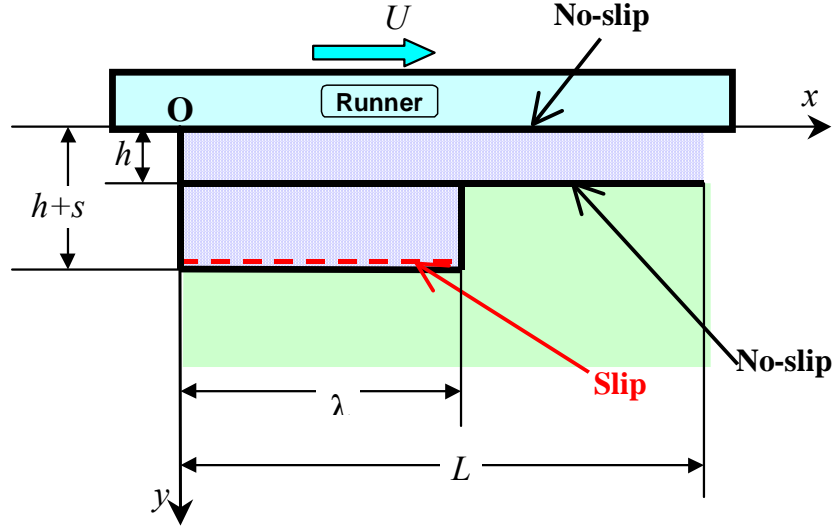


Figure 3 – Location of the slip/no-slip zones

For case B, total slip on the bottom surface of the dimples, requires the following boundary condition:

$$\left. \frac{du}{dy} \right|_{y=h+s} = 0 \quad (9)$$

Consequently, flow rate in x direction in the slip zone will be:

$$Q_s = \lambda U(h+s) - \frac{\lambda(h+s)^3}{3\eta} \frac{dp}{dx} \quad (10)$$

Flow rate conservation (of Couette and Poiseuille components) for an entire cell can be written in a condensed manner introducing the variable γ that counts for slip condition:

$\gamma = 1$ no-slip condition - case A, respectively

$\gamma = 2$ total-slip condition - case B.

$$\begin{aligned} \frac{\lambda U}{2} [\gamma(h+s) - h] &= \frac{\gamma^2 \lambda (h+s)^3 (p_m + (1-A)p_b)}{12\eta\lambda} + \\ &+ \frac{\lambda h^3 (p_m - Ap_b)}{12\eta(L-\lambda)} + \frac{(L-\lambda)h^3}{12\eta} \left[\frac{p_m + (1-A)p_b}{\lambda} + \frac{p_m - Ap_b}{L-\lambda} \right] \end{aligned} \quad (11)$$

Now, introducing equations (3), (4) and (8) into equation (11) we obtain the raw maximum pressure (without cavitation effects):

$$\bar{p}_{max} = \frac{p_{max} h^2}{\eta U L_{tot}} = \frac{6\beta N(\gamma H - 1)(1-\Lambda)}{\left[\gamma^2 H^3 (\Lambda N + \beta - \Lambda) + N(1-\Lambda) + \frac{6\Lambda(N + \beta - \Lambda)}{6-5\Lambda} \right] \left(N + \beta - \frac{\Lambda}{2} \right)} \quad (12)$$

The correction necessary to reach the maximum pressure p_{max}^r is found from the similitude of the triangles $\Delta OO'G$ and $\Delta A''BC$ (see Figure 2):

$$p_c = p_{max}^r \frac{A}{2\beta} \quad (13)$$

As $p_{max} = p_{max}^r + p_c$, results:

$$p_{max}^r = p_{max} \frac{2\beta}{2\beta + \Lambda} \quad (14)$$

Consequently:

$$\bar{p}_{\max}^r = \frac{p_{\max}^r h^2}{\eta U L_{\text{tot}}} = \frac{C_1(\gamma H - 1)}{\gamma^2 H^3 C_2 + C_3} \quad (15)$$

where:

$$C_1 = \frac{12\beta^2 N(1-\Lambda)}{(N + \beta - 0.5\Lambda)(2\beta + \Lambda)}; \quad C_2 = \Lambda(N-1) + \beta \quad \text{and}$$

$$C_3 = N(1-\Lambda) + \frac{6\Lambda(N + \beta - \Lambda)}{6 - 5\Lambda}$$

The ratio of the two values of the maximum pressure corresponding to the two cases (with total slip on the bottom of the dimples and without slip) is:

$$R = \frac{(2H-1)(H^3 C_2 + C_3)}{(H-1)(4H^3 C_2 + C_3)} \quad (16)$$

Analyzing equation (16), we may conclude that for $H \rightarrow 1$, $R \rightarrow \infty$, respectively that in the case with slip on the bottom of the dimples, the maximum pressure is strictly positive, while in the no-slip case there is no hydrodynamic pressure generated for $H = 1$ (flat and parallel surfaces). The variation of the maximum dimensionless pressure, \bar{p}_{\max} , as function of the dimensionless film thickness, H , for the two different sets of boundary conditions (slip and no-slip) will be discussed in Chapter 4.

3. NUMERICAL SOLUTION

A 2-D finite difference flow model was developed in order to validate the analytical solution.

The equations solved are the Reynolds equation, which for parallel surfaces becomes Laplace equation, and the continuity of the flow at the discontinuities. Boundary conditions are zero-pressure at slider front and rear edges and zero pressure gradients on each side.

The system of equations was solved using the Gauss-Seidel method with over-relaxation. All sub-ambient pressures are set to zero at every iteration, so the Reynolds continuity condition is preserved.

In order to verify the convergence of the solution, several sets of meshing were tested. Finally, a number of 20 mesh point for each cell were used, a good compromise between computation time and numerical accuracy.

In order to have alternative numerical results a 3D flow model was solved using a commercially available software (FLUENT). The validation was performed on sliders with a small number of dimples, N . Despite some limitations, we have also included FLUENT cavitation algorithm to qualitatively study the influence of this phenomenon on the main performance characteristics.

A typical comparison of the analytical model and both numerical models, in terms of longitudinal pressure distribution in the midplane, is presented in Figure 4. The partially textured slider analyzed had the following input data: $L_{\text{tot}}=1.2\text{mm}$, $h=3\mu\text{m}$, $s=3\mu\text{m}$, $N=3$, $\alpha=0.5$, $\eta=0.3\text{Pa}\cdot\text{s}$, $U=1\text{m/s}$. The results, only for case A (No-slip boundary condition), are presented considering two different texture densities ($\rho=0.25$ and $\rho=0.64$).

As can be seen in Figure 4, there is a good agreement between the three sets of results, especially for high texture densities.

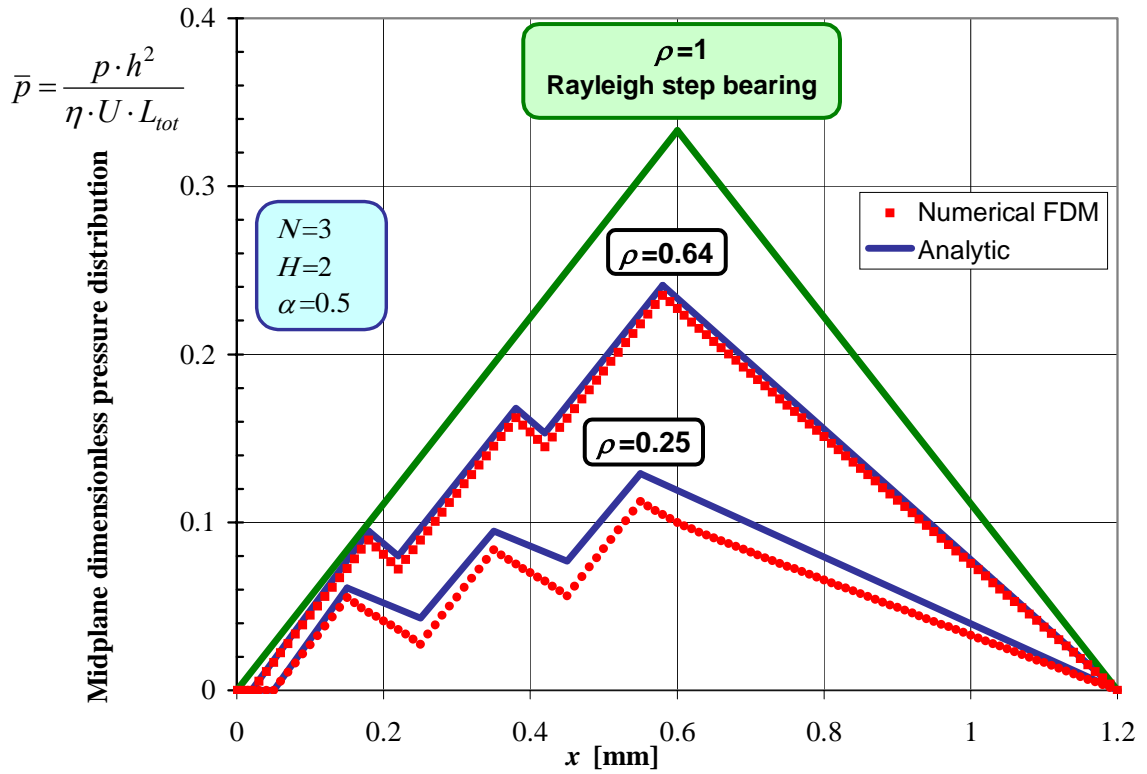


Figure 4 – Pressure distribution in the midplane of the slider (No-slip condition)

It is interesting to remark that when texture density reaches its maximum limit ($\rho \rightarrow 1$) the pressure distribution becomes identical with that of a classical Rayleigh step bearing. For the particular case plotted in Figure 4 the maximum dimensionless pressure is $\bar{p}_{max} = 1/3$, which is the value obtained for corresponding stepped slider. This is explained by the fact that when the dimples occupy the entire surface, the slider becomes a stepped slider.

4. RESULTS

The encouraging results obtained after analytical vs. numerical model comparison allow the parametric analysis of the main performance characteristic of the slider, namely the maximum dimensionless pressure, \bar{p}_{max} . In the following graphs are also included numerical results obtained with the finite differences model, in order to extend the validation of the analytical model.

The parametric analysis is performed for slip (case A), respectively, no-slip (case B) conditions, in terms of the following four dimensionless parameters: N , ρ , H , α .

For the sake of clarity two relationships are mentioned:

$$A = 1 - \sqrt{\rho} \quad \text{and} \quad \beta = N \frac{1 - \alpha}{\alpha} + \frac{\Lambda}{2}$$

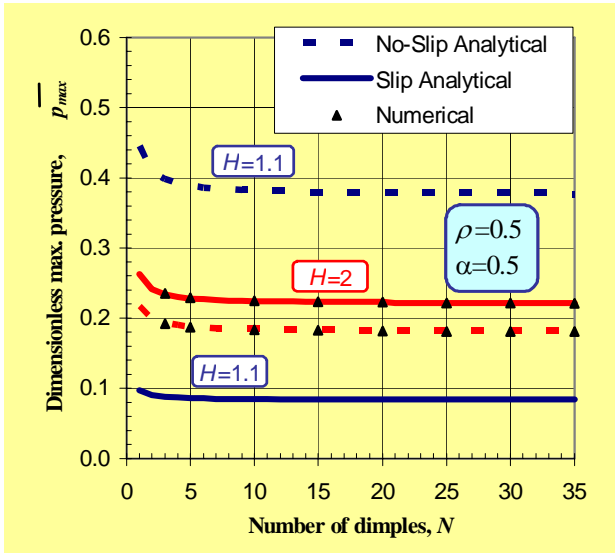


Figure 5.

In Figure 5, the influence of the number of dimples, N , on the maximum dimensionless pressure for two values of film ratio ($H=1.1$ and $H=2$), is presented. The texture density is $\rho=0.64$, and the textured fraction is $\alpha=0.5$. One can remark that the maximum pressure decreases asymptotically with N ; however is practically constant for typical textured sliders where $N > 5$. This conclusion is valid for both boundary condition cases A and B.

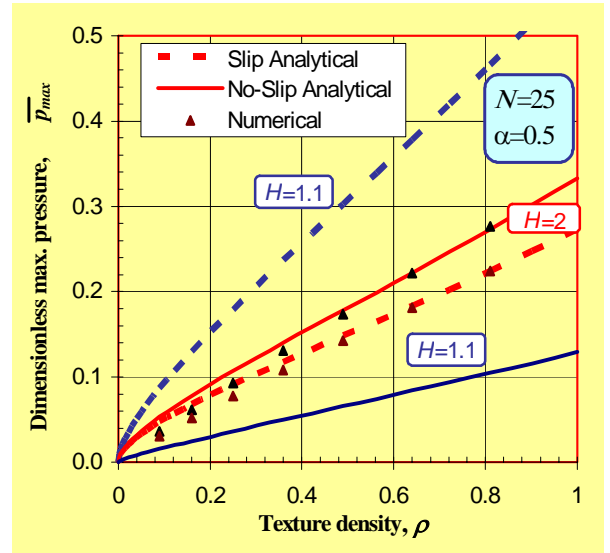


Figure 6.

In Figure 6 the influence of the texture density, ρ , on the maximum dimensionless pressure is plotted for $N=25$, $\alpha=0.5$, and two film ratios ($H=1.1$ and $H=2$). The pressure increases almost linearly with the density, ρ .

The influence of the dimensionless film thickness on the maximum dimensionless pressure is presented in Figure 7, for three different densities: $\rho=0.49$, $\rho=0.64$, $\rho=0.81$. The same textured slider with $N=25$ and $\alpha=0.5$ was considered for both boundary condition cases.

One can remark the existence of a maximum for maximum pressure located around $H=1.7$ for No-slip conditions (case A). This optimum film ratio is very similar to that of the Rayleigh step bearing. Analogously, the optimal film thickness ratio in case B (slip condition) is close to $H=1$.

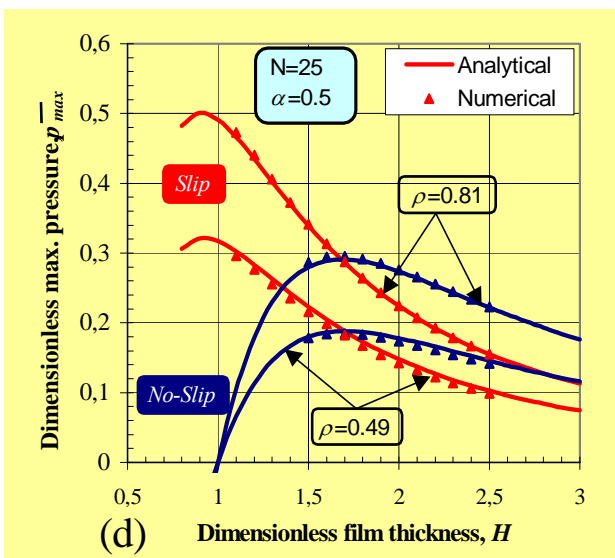


Figure 7.

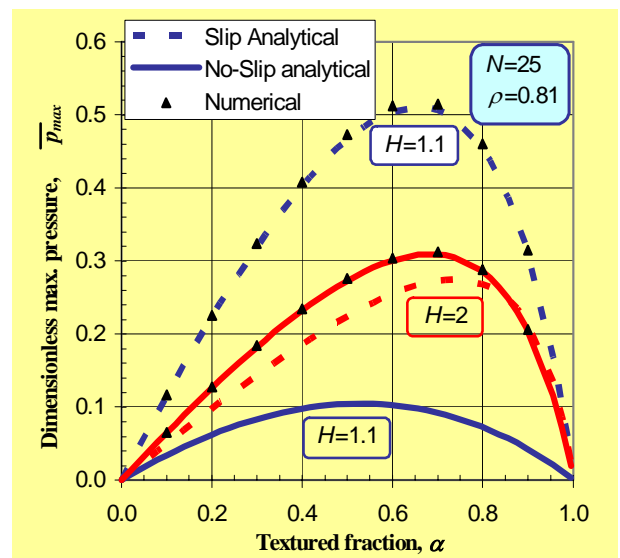


Figure 8.

Analyzing Figure 7, one can also conclude:

- The overall maximum pressure and correspondingly, the maximum lift force for case B (with local slip) are substantially greater than that in case A (No-slip).
- The decrease of the maximum pressure with H is sharper for case B and thus for $H > 1.75$ the lift force generated is greater in case A (No-slip).
- In case B (with local slip) the maximum lift force is obtained for a dimensionless film thickness $H \sim 1$. This shows that heterogeneous surface treatment (“pseudotexturing”) ensures operation with optimum load capacity regardless film thickness value [9]. This is not the case for “real” textured slider. Obviously, the load capacity is proportional with the inverse of the square of the film thickness.

Finally, in Figure 8 the influence of the textured fraction α on the maximum pressure is presented for $N=25$, $\rho=0.81$, and two distinct values of film thickness ratio: $H=1.1$ and $H=2$. One can remark the existence of an extreme value of the maximum pressure corresponding to $\alpha > 0.5$.

5. CONCLUSIONS

The original analytical model for pressure distribution calculation in a partially textured slider has been successfully compared with numerical 2D & 3D models.

A parametric study of maximum pressure was performed and optimal texture parameters have been found.

- The dimple density as large as possible. The maximal dimple density depends on the manufacturing technology adopted.
- The textured fraction $\alpha \sim 0.7$.
- The dimensionless film thickness $H \sim 1.7$ for case A and $H \sim 1$ for the second case (with local slip). The last value is very important: regardless of film thickness, operation occurs with optimal load capacity.

The partially textured slider has lower load carrying capacity than a stepped slider, but can be more easily manufactured by various technologies (e.g. lithography).

ACKNOWLEDGEMENTS

Financial support for the work described in this paper was provided by National Council for Academic Scientific Research (CNCSIS) under Grants No. 1418/2004 and 464/2004. The authors express their gratitude to Associate Professor Traian CĂCONE for his precious help.

REFERENCES

- [1] Brizmer V., Klingerman, Y., Etsion, I., *A laser surface textured parallel thrust bearing*, Tribology Transactions, Vol. 46, No 3, pp. 397-403, 2003.
- [2] Burstein, L., Ingman, D., *Effect of pore ensemble statistics on load support of mechanical seals with pore-covered faces*, Journal of Tribology, Vol. 121, pp. 927-932, 1999.
- [3] Etsion, I., *A laser surface textured hydrostatic mechanical seal*, Tribology Transactions, Vol. 45, No 3, pp 430-434, 2002.
- [4] Etsion, I., Burstein, L, *A model for mechanical seals with regular microsurface structure*, Tribology Transactions, Vol. 39, No. 3, pp. 677-683, 1996.
- [5] Etsion, I., Halperin, G., Brizmer, V., Klingerman, Y., *Experimental investigation of laser surface textured parallel thrust bearings*, Tribology Letters, Vol.17, No.2, August 2004.
- [6] Etsion, I., Klingerman, Y., *Analytical and experimental investigation of laser-textured mechanical seal faces*, Tribology Transactions, Vol. 42, No. 3,pp. 511-516, 1999.
- [7] Golloch, R., Merker, G.P., Kessen, U., Brinkmann, S., *Benefits of laser-structured cylinder liners for internal combustion engines*, 14th International Colloquium Tribology, Esslingen, Germany, Vol.1, pp. 321-328, 2004
- [8] Hamilton, D.B., Walowit, J.A., Allen, C.M., *A Theory of Lubrication by Micro-irregularities*, ASME-ASLE Lubrication Conference, October 18-20 Paper No. 65-Lub-11, 1965.
- [9] Hild W., Opitz A., Schaefer J. A., Scherge M., *The effect of wetting on the microhydrodynamics of surfaces lubricated with water and oil*, Wear, Vol. 254, pp 871-875, 2003.
- [10] Ronen, A., Etsion,I., Klingerman, Y., *Friction-reducing surface-texturing in reciprocating automotive components*, Tribology Transactions, Vol. 44, No. 3, pp. 359-366, 2001.
- [11] Ryk, G., Klingerman, Y., Etsion, I., *Experimental investigation of laser surface texturing for reciprocating automotive components*, Tribology Transactions, Vol. 45, No. 4, pp. 444-449, 2002
- [12] Salant R. F., Fortier A. E., *Numerical simulation of a slider bearing with an engineered slip/no-slip surface*, 14th International Colloquium of Tribology, Esslingen, Germany, Vol. 3, pp. 1699-1704, 2004.
- [13] Zhu Y., Granick S., *Rate-dependent slip of Newtonian liquid at smooth surfaces*, Physical review letters, Vol. 87, No. 9, pp. 096-105, 2001